"Sweet" Ionic Liquid Gels: Materials for Sweetening of Fuels

Gunaratne, H., Plechkova, N., & Seddon, K. (2018). "Sweet" Ionic Liquid Gels: Materials for Sweetening of Fuels. *Green Chemistry*, *20*, 1-19. https://doi.org/10.1039/C8GC01615A

Published in:
Green Chemistry

Document Version:
Peer reviewed version

Green Chemistry

Accepted Manuscript

This article can be cited before page numbers have been issued, to do this please use: F. Billeci, F. D'Anna, H. Q. N. Gunaratne, N. V. Plechkova and K. R. Seddon, *Green Chem.*, 2018, DOI: 10.1039/C8GC01615A.

ROYAL SOCIETY OF CHEMISTRY

rsc.li/green-chem

View Article Online
DOI: 10.1039/C8GC01615A

Journal Name

ARTICLE

"Sweet" Ionic Liquid Gels: Materials for Sweetening of Fuels

Floriana Billeci,[a] Francesca D'Anna,[a]* H. Q. Nimal Gunaratne,[b,c] Natalia V. Plechkova,[b] Kenneth R. Seddon[b,d]

Received 00th January 20xx,
Accepted 00th January 20xx

DOI: 10.1039/x0xx00000x

www.rsc.org/

The search for new materials to be used in desufurisation (sweetening) of fuels is one of the main topics of the current research. In this paper, we explored the possibility of using supramolecular gels obtained from the gelation of ionic liquid binary mixtures. Indeed, some ionic liquids generally are known as efficient extraction phases for desulfurisation of fuels. In rare cases, one of the main drawbacks is their partial solubility in the fuel leading to contamination. Then, their immobilisation due to the formation of a gelatinous network may be a challenge. Ionic liquid gels were obtained by mixing certain [NTf_2^-]-based ionic liquids (solvents) with the ones of gluconate-based ionic liquids (gelators). Our gelators are derived from renewable sugar which possess the marked ability to form hydrogen bonds highly favouring gel formation. In this work, for the first time, ionic liquid gels were used to adsorb typical sulfur compounds omnipresent in fuels. Aromatic sulfur contaminants like thiophene, benzothiophene and dibenzothiophene were selected as model compounds. Our ionogels proved efficient adsorption phases, particularly in the removal of benzo- and dibenzothiophenes usually claimed as refractory compounds for both extraction and oxidative desulfurisation processes. The adsorption efficiency was barely affected by volume, but significantly depended on the fuel concentration.

Introduction

Sustainability is one of the most important challenges of the modern society.[1] Its main goal is the development of safer and more environmentally friendly processes that integrate the needs of economic competitiveness and societal concerns. In this context, search and development of new methods and liquid fuels play a pivotal role. Indeed, liquid fuels with omnipresent sulfur compounds give rise to the formation of oxyacids as a result of combustion. These cause environmental and industrial concerns.[2] The detrimental effects of sulfur compounds on automobile engines and fuel cells are well documented.[2] All the above drawbacks justify the severity of the actual regulations to adjust the permissible sulfur concentration in fuels to about 10 ppm.[3]

The most important approach to lower sulfur level in fuels is the hydrodesulfurisation process that since the 1930s features the manufacturing of fuels.[2] Although this process proved quite efficient, it is less successful in the removal of aromatic sulfur compounds and, in particular of benzothiophene derivatives as a consequence of their low reactivity. This is the reason why different methods like oxidative, biological, adsorptive and extractive desulfurisation have been taken into account.[4-7] Obviously, regardless of methodology, the materials used in this process should possess low toxicity, efficient reusability and low costs.

As far as adsorption methods are concerned, different solid sorbents such as carbon beads,[8] graphene oxides,[9] functionalised polymers,[10, 11] metal oxides[12] *etc.* have been used.

However, to the best of our knowledge, the possibility of using gel phases and, in particular, supramolecular gels for desulfurisation has never been explored. Why could these materials be advantageous? Firstly, it is well known that they are formed through self-assembly processes, occurring in different media like water, organic solvents or ionic liquids (ILs) with low molecular weight compounds also called gelators (LMWGs).[13-16] These latter, with respect to polymeric gelators, have the advantage to be more easily tailored for specific applications and could be prepared in the light of the "biorefinery concept", firstly introduced by John and coworkers.[17, 18] This proposes the possibility that gelators wholly occur from natural sources or they are prepared using naturally occurring reagents. Furthermore, these soft materials are highly porous and exhibit pronounced adsorption abilities that have widely favoured their use as smart materials for pollutant removal.[19, 20]

All the above advantageous aspects could be further improved, if alternative and eco-friendly solvents, that are highly efficient in extractive desulfurisation like ILs,[21-27] would

[a] *Dipartimento STEBICEF, Università degli Studi di Palermo, Viale delle Scienze, Ed. 17, 90128 Palermo (Italy); email: francesca.danna@unipa.it*
[b] *QUILL Research Centre, School of Chemistry and Chemical Engineering, Queen's University of Belfast, Stranmillis Road, Belfast BT9 5AG, U.K.*
[c] *School of Chemistry and Chemical Engineering, Queen's University, Belfast BT9 5AG, UK*
[d] *deceased.*

Electronic Supplementary Information (ESI) available: [synthetic details; DSC and TGA traces, strain sweep measurements, RSL and opacity measurements; NMR measurements; tables of gelation tests, tables of adsorption efficiency]. See DOI: 10.1039/x0xx00000x

View Article Online
DOI: 10.1039/C8GC01615A

form gelatinous matrix. Such ionic liquid gels (ILGs) combine the abilities of ILs with the ones of a solid-like phase, which could be easier to handle than a liquid one.[16, 28-32]

Literature reports on ILs so far indicate that they are able to self-organise in conventional solvents, for example, surfactants and liquid crystals.[33] However, in a binary mixture and under suitable conditions, a gel phase could be formed. So, one IL will be responsible for the fibrillary network formation, whereas the other one, present in excess, will be the immobilised phase.[20, 29, 30, 34]

In all cases, important properties of ILs, like charge transport,[35] catalytic activity[36] and electrical conductivity[36] are improved.

With all this in mind, we explored the possibility of using ILGs as sorbents for desulfurisation of fuels. For this purpose, we took into consideration gelation of some phosphonium and ammonium organic salts, namely the trihexyltetradecylphosphonium gluconate (**[P_{66614}][Glu]**), tetrabutylphosphonium gluconate (**[P_{4444}][Glu]**) and tetrabutylammonium gluconate (**[N_{4444}][Glu]**)(Scheme 1) in aliphatic ILs.

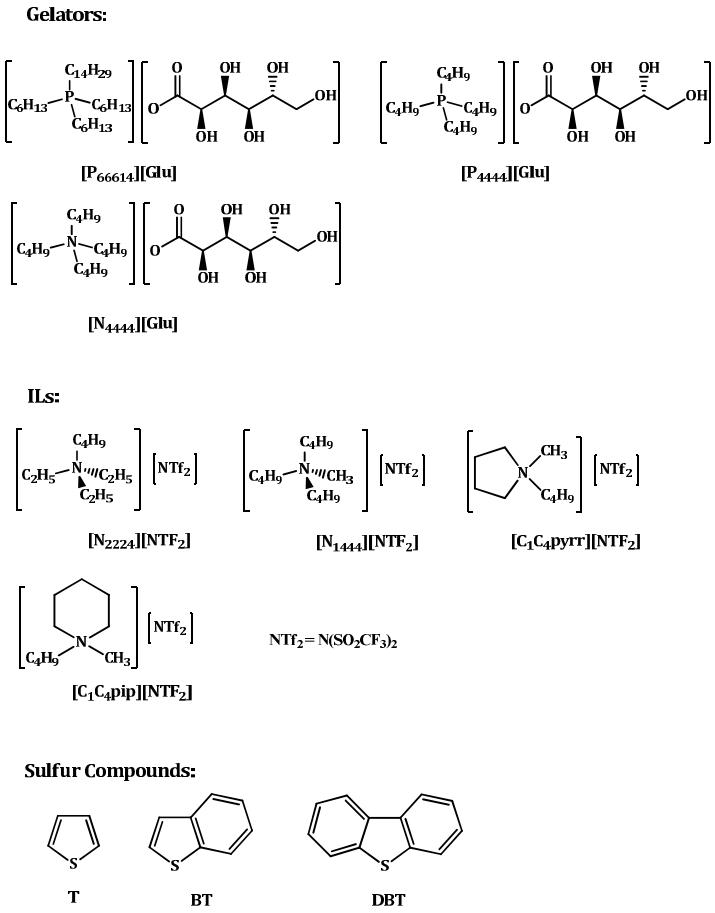

Scheme 1. Structures of gelators, ILs and sulfur compounds used in this study.

Recent reports have claimed the efficiency of phosphonium ILs in extractive desulfurisation of fuels.[37] In our study, all gelators have the gluconate anion that is derived from natural sources and is known for its low toxicity.[38] Moreover, the presence of hydroxyl groups should favour the formation of the 3D-network of the gel phase. Finally, we preferred aliphatic cations over aromatic to minimise toxicity and enhance performance of our materials.[39] Our gelators are characterised by the presence of alkyl chains of different length to assess the rôle played by van der Waals interactions in determining the properties of gel phases.

As solvents, $[NTf_2]^-$ ILs with various cation structures were chosen. In particular, the effects deriving from the presence of different alkyl chain lengths ($[N_{2224}]^+$ and $[N_{1444}]^+$), as well as cyclic cations with different size and flexibility ($[C_1C_4pyrr]^+$ and $[C_1C_4pip]^+$), were taken into consideration.

After preliminary gelation tests, ILGs thus obtained were characterised determining the critical gelation concentration (CGC), *i.e.* the minimal amount of gelator needed to have gel formation and the temperature corresponding to gel-sol transition (T_{gel}).

Gel phase formation was studied as a function of time, using opacity and resonance light scattering (RLS) measurements. Mechanical properties of soft materials were assessed by rheology investigation, whereas to deepen the understanding about the organisation and interactions involved in the 3D-network, we performed ^{1}H NMR investigation in the

View Article Online
DOI: 10.1039/C8GC01615A

temperature range 293-373 K and recorded FT-IR spectra of both ILs and ILGs.

Soft materials were analysed also for their ability to self-repair after the application of external stimuli, such as magnetic stirring and ultrasound irradiation, whereas their morphology was observed by polarised optical microscopy (POM). After the determination of soft materials properties, we studied their utilisation for the removal of thiophene (**T**), benzothiophene (**BT**) and dibenzothiophene (**DBT**) from a hexane solution, a system frequently used to mimic liquid fuel.[40, 41] To fulfil this aim, important parameters like temperature, adsorption time, volume and concentration of fuels, ability of multiextraction (mixture of S-compounds), contact surface area and the possibility of reusing the gel phase were analysed. Data collected show that our ILGs exhibit a good adsorption efficiency towards benzo- and dibenzothiophene that generally are more refractory to desulfurisation processes. Furthermore, our results also demonstrate that these sorbent systems may be reused for at least three cycles maintaining good levels of efficiency.

Results and Discussion

Synthesis of gluconate ionic liquids

Our organic salts were prepared by equimolar acid-base reaction of the corresponding ammonium and phosphonium hydroxides with gluconic acid (Scheme 2).

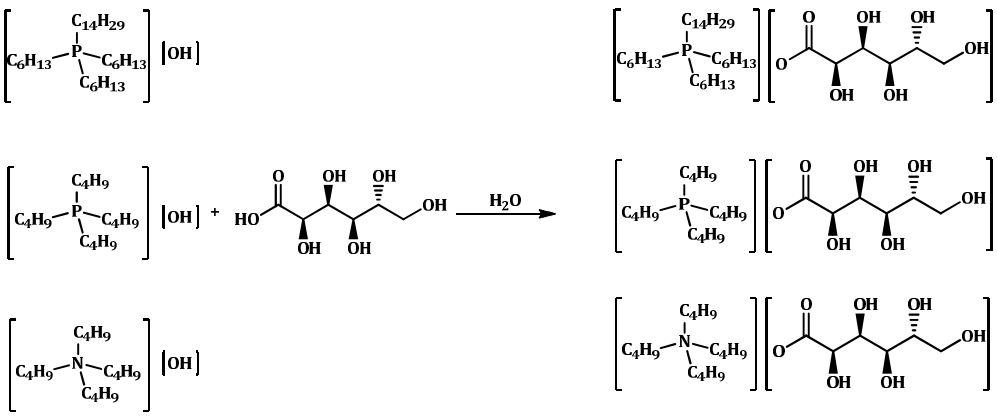

Scheme 2. Representation of synthetic procedure.

In the case of $[P_{6\,6\,6\,14}][Glu]$, the hydroxide was obtained by anion exchange on resin, using a procedure previously reported in literature.[33] Full compound characterisation is reported in ESI.

Thermal behaviour. The thermal behaviour of our salts was investigated by DSC and TGA measurements. Traces of heat-cool cycles are reported in Figure S1.

In all cases, in the heating cycle, we observed transitions that were ascribed to melting processes. The melting temperatures and enthalpies were determined from the maximum of the signal and its area, respectively. With the only exception of **$[P_{4\,4\,4\,4}][Glu]$**, in the cooling cycle, we observed transitions ascribed to crystallisation process. In all cases, transitions observed were reproducible in the second cycle.

In Table 1, the melting and crystallisation temperatures (T_m and T_c), corresponding enthalpies (ΔH_m and ΔH_c) and entropies (ΔS_m and ΔS_c) are reported.

Table 1. Temperature and thermodynamic parameters associated with the melting and crystallisation processes (T_m, ΔH_m, ΔS_m, T_c, ΔH_c and ΔS_c) obtained by DSC measurements. Temperatures corresponding to the onset of decomposition (T_d) obtained by TGA analysis.

Salt	T_m (°C)	ΔH_m (J/g)	ΔS_m (J/g K)	T_c (°C)	ΔH_c (J/g)	ΔS_c (J/g K)	T_d (°C)
$[N_{4\,4\,4\,4}][Glu]$	134.9	105.3	0.26	73.4	-86.4	-0.25	161.80
$[P_{4\,4\,4\,4}][Glu]$	81.5	78.7	0.22	-	-	-	155.04
$[P_{6\,6\,6\,14}][Glu]$	35.6	21.2	0.069	0.48[a]	-28.1[a]	-0.10[a]	172.51

[a]Obtained from the second cycle

Firstly, the comparison between T_m values measured for gluconate salts with the ones previously reported for the corresponding chloride salts (T_m = 52, 62 and -70 °C for $[N_{4\,4\,4\,4}]Cl$, $[P_{4\,4\,4\,4}]Cl$ and $[P_{6\,6\,6\,14}]Cl$, respectively)[42, 43] shows how the presence of gluconate anion induces a significant

View Article Online
DOI: 10.1039/C8GC01615A

increase in T_m, as a consequence of the increased ability to establish hydrogen-bonded networks.

In general, T_m decreases on going from ammonium to phosphonium salts and, among the salts used, only phosphonium salts were able to behave as ILs, having T_m lower than 100 °C.[44] This result indicates the rôle played by the nature of the central atom of the cation (N or P) in determining the solid lattice organisation. Analysis of corresponding thermodynamic parameters shows that differences observed in T_m values are mainly due to the strength of cation-anion interactions rather than differences in the organisation of the solid lattice. Indeed, the most significant changes were detected in ΔH_m rather than in ΔS_m values.

As expected, a shorter alkyl chain and symmetric structure determine a higher T_m for **[P$_{4444}$][Glu]** than for **[P$_{66614}$][Glu]**. Moreover, the lengthening of the alkyl chain gives rise to weaker cation-anion interactions and a lower organisation in the solid state.

The melting of salts was also observed using POM. In all cases, melting gave rise to isotropic solutions, and interesting textures were exhibited during both heating and cooling cycles (Figure 1).

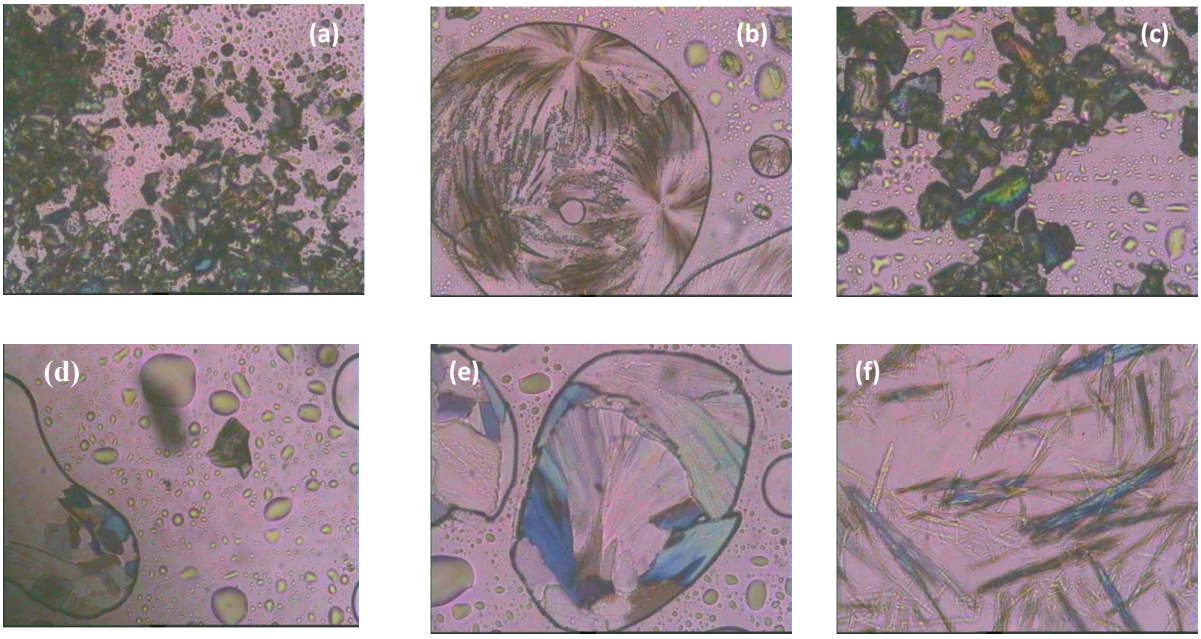

Figure 1. POM images corresponding to (a) **[N$_{4444}$][Glu]** at 120 °C, heating cycle; (b) **[N$_{4444}$][Glu]** at 115.8 °C, cooling cycle; (c) **[P$_{4444}$][Glu]** at 68.1 °C, heating cycle; (d) **[P$_{4444}$][Glu]** at 34.4 °C, cooling cycle; (e) **[P$_{4444}$][Glu]** at 43.8 °C, second heating cycle; (e) **[P$_{66614}$][Glu]** at 32.1 °C, heating cycle.

For example, in the case of **[N$_{4444}$][Glu]**, until 120 °C, the presence of discrete crystals was detected (Figure 1a). After melting, followed by cooling of the isotropic solution exhibited well organised and oriented spherulitic structures at 115.8 °C that persisted also at 36 °C (Figure 1b).

A similar behaviour was observed for **[P$_{4444}$][Glu]**. Indeed, also in this case until 68.1 °C, the presence of coloured crystals was detected (Figure 1c). During the first cooling cycle at 34.4 °C (Figure 1d), non-isotropic liquid was obtained with changes in the brightness and coloured crystals. In general, similar behaviours have been previously reported analysing melting processes of some N-alkylcaprolactam ILs.[45]

However, the lengthening of the alkyl chain in the **[P$_{66614}$][Glu]**, softens all the above phenomena and, until 32.1 °C, we detected the occurrence of filamentary coloured structures (Figure 1f) that definitely disappeared after melting.

As for the thermal stability of gluconate salts, the temperatures corresponding to the onset of decomposition (5% of weight loss; T_d) are reported in Table 1 (Figure S2). Trend in T_d values shows that, alkyl chain length being the same and thermal stability decreases on going from ammonium to phosphonium salts. On the other hand, for phosphonium salts, the lengthening of the alkyl chain induces a significant increase in thermal stability.

Gelation tests and gel-sol transition temperature determination. The salts synthesised were tested for their gelling ability. For this, we used several solvents differing in polarity and viscosity, including organic solvents, oils, ILs and water (Table S1).

To perform gelation tests, we applied the heating/cooling method. Firstly, the solvent plus gelator mixture was heated until a clear solution was obtained. Then, it was left staying at 4 °C overnight. Using the tube inversion test,[46, 47] we assessed the gel phase formation.

View Article Online
DOI: 10.1039/C8GC01615A

Salts were soluble at room temperature in protic polar solvents, such as alcohols and water. As far as oils are concerned, salts resulted soluble in hot olive oil, sweet corn oil and engine oil. Conversely, they were insoluble in silicone oil, mixed seed oil and diesel. Finally, as for low polar organic solvents, salts proved insoluble in hot cyclohexane. On the grounds of the above results, we decided to test their behaviour in IL solutions.

In particular, paying attention to the environmental impact of solvents used, we favoured aliphatic rather than aromatic ILs using $[N_{2\,2\,2\,4}][NTf_2]$, $[N_{1\,4\,4\,4}][NTf_2]$, $[C_1C_4pip][NTf_2]$ and $[C_1C_4pyrr][NTf_2]$. Salts showed different behaviour as a function of ILs used. **$[P_{6\,6\,6\,14}]$[Glu]** exhibited the best gelling ability giving gels in all ILs tested. Differently, **$[P_{4\,4\,4\,4}]$[Glu]** gave gel phases only in ammonium-based ILs, whereas **$[N_{4\,4\,4\,4}]$[Glu]** gelled only in $[N_{1\,4\,4\,4}][NTf_2]$. In all cases, we obtained white and thermoreversible opaque gels that resulted stable for at least four months (Figure 2).

Figure 2. Picture of **$[P_{4\,4\,4\,4}]$[Glu]/ $[N_{2\,2\,2\,4}]$[NTf$_2$]** ILG.

For all gel phases, we determined the CGC and the T_{gel} that was firstly determined by the lead-ball method[48] (Table 2).

Table 2. CGC and $T_{gel\text{-}CGC}$ corresponding to gel phases obtained. $T_{gel\text{-}6.5\%\ wt}$, sol-gel temperature ($T_{c\text{-}6.5\%wt}$), gel-sol and sol-gel enthalpy (ΔH_m and ΔH_f) determined for gel phases at 6.5% wt by DSC measurements.

IL	Gelator	CGC /wt%	$T_{gel\text{-}CGC}$/°C[a]	$T_{gel\text{-}6.5\%wt}$ /°C	ΔH_m/Jg^{-1b}	$T_{c\text{-}6.5\%wt}$ /°C	ΔH_c Jg^{-1b}
$[N_{2\,2\,2\,4}][NTf_2]$	$[P_{6\,6\,6\,14}]$[Glu]	3	29	25[a] 30.1[b]	1.72	3.51	1.43
	$[P_{4\,4\,4\,4}]$[Glu]	5	21	22[a]			
$[N_{1\,4\,4\,4}][NTf_2]$	$[P_{6\,6\,6\,14}]$[Glu]	5.5	23	26[a] 18.2[b]	44.6		
	$[N_{4\,4\,4\,4}]$[Glu]	5	20	21[a] 13.7[b]	22.1		
	$[P_{66614}]$[Glu]	5.5	23	26[a] 18.2[b]	3.49	-5.76	0.94
$[C_1C_4pip][NTf_2]$	$[P_{66614}]$[Glu]	5	25	27[a] 20.9[b]	1.41		
$[C_1C_4pyrr][NTf_2]$	$[P_{66614}]$[Glu]	5	25	28[a] 24.6[b]	2.46		

[a]Determined by the lead-ball method.[48] T_{gel} were reproducible within ± 1 °C. [b]Determined by DSC.

CGCs range 2-5.5% and T_{gel}s at CGC change between 20 and 29 °C. Taking into consideration our best gelator, **$[P_{6\,6\,6\,14}]$[Glu]**, we observed a significant increase in CGC on going from $[N_{2\,2\,2\,4}][NTf_2]$ to $[N_{1\,4\,4\,4}][NTf_2]$. This is coupled with a decrease in T_{gel}.

$[P_{4\,4\,4\,4}]$[Glu] shows the opposite behaviour. The observed trend indicates a complementary effect operating between the IL and gelator's alkyl chain length, probably ascribable to the extent of van der Waals interactions established in the gelatinous network. On the other hand, changing the geometry of IL cation, in the case of $[C_1C_4pip][NTf_2]$ and $[C_1C_4pyrr][NTf_2]$, does not affect the gelation ability.

Finally, the different nature of gelator cation (ammonium or phosphonium) significantly affects gelling ability, as accounted for by the increase in CGC and decrease in T_{gel} detected on going from **$[N_{4\,4\,4\,4}]$[Glu]** to **$[P_{4\,4\,4\,4}]$[Glu]**.

T_{gel}s were also determined at the common concentration of 6.5% wt to draw a comparison among different soft materials obtained (Table 2). The same concentration was used to perform the full gel characterisation. In this case, measurements were carried out using both DSC and the lead-ball method.[48] These two methods observe different situations, *i.e.* the initial loss of consistency of the gelatinous network, in the case of the lead-ball method, and its complete breakdown in the case of DSC investigation (Figure S3).

Comparison with T_{gel} collected at the CGC shows that the increase in concentration barely affects this parameter. Furthermore, in most cases, $T_{gel\text{-}6.5\%\ wt}$ determined by DSC were lower than the ones detected by the lead-ball method.

We were unable to obtain the DSC thermogram of **$[P_{4\,4\,4\,4}]$[Glu]/$[N_{2\,2\,2\,4}]$[NTf$_2$]** gel due to instrumental limitation. On the other hand, in the cases of **$[P_{6\,6\,6\,14}]$[Glu]/$[N_{2\,2\,2\,4}]$[NTf$_2$]**

View Article Online
DOI: 10.1039/C8GC01615A

and **[P_{4444}][Glu]/[N_{2224}][NTf_2]**, during the cooling cycles, gel phase formation was observed. In both cases, $T_{c\text{-}6.5\%\ wt}$ were significantly different from the melting temperature, indicating that hysteresis phenomena occured.

Gel transition temperatures were obtained by DSC range from 13.7 up to 30.1 °C. In general, trends detected for $T_{gel\text{-}6.5\%\ wt}$ perfectly recall those above discussed for CGCs. Indeed, as far as gels in [N_{1444}][NTf_2] are concerned, temperature decreases on going from **[P_{4444}][Glu]** to **[P_{66614}][Glu]**.

Finally, DSC measurements account for an effect deriving from the geometry of IL cation, as demonstrated by the increase in $T_{gel\text{-}6.5\%\ wt}$ on going from **[P_{66614}][NTf_2]/[C_1C_4pip][NTf_2]** to **[P_{66614}][Glu]/[C_1C_4pyrr][NTf_2]**.

POM investigation of gels. Full gel characterisation was performed using 6.5% wt of gelator. Firstly, morphology of ILGs was observed as a function of temperature by POM. For all gel phases, heating at a much higher temperature than the melting one gave isotropic solutions. In all cases, as a consequence of the thermoreversibility of materials, cooling of isotropic solutions at room temperature allowed observing the appearance of aggregates featuring the gel phase. In Figure 3, POM images collected for gels obtained as a function of different gelators and ILs, are shown.

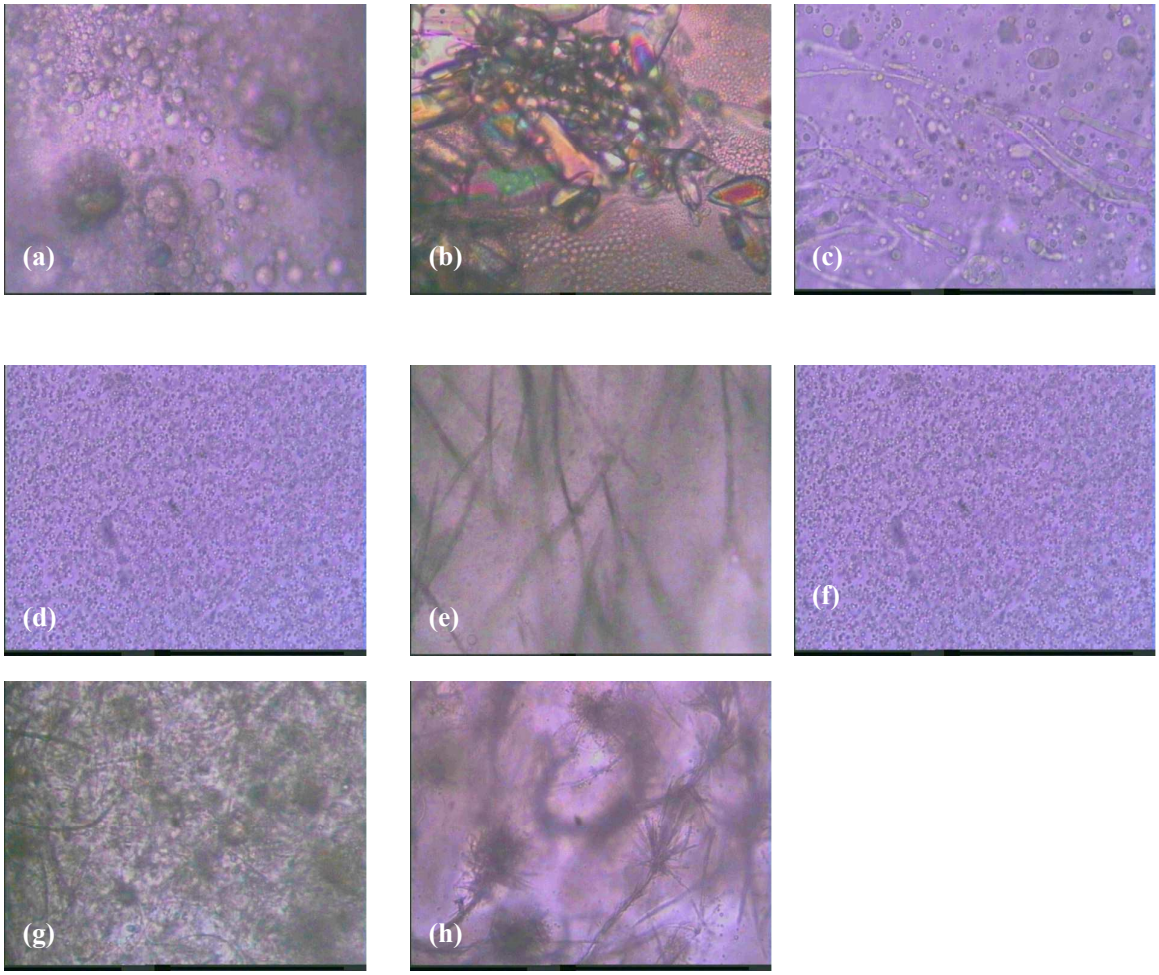

Figure 3. POM images of ILGs at 6.5% wt of gelator for: (**a**) **[N_{4444}][Glu]/[N_{1444}][NTf_2]** at 25.7 °C on heating; (**b**) **[N_{4444}][Glu]/[N_{1444}][NTf_2]** 35.7 °C on cooling; (**c**) **[P_{4444}][Glu]/[N_{1444}][NTf_2]** at 24.4 °C on heating; (**d**) **[P_{4444}][Glu]/[N_{1222}][NTf_2]** at 23.1 °C on heating; (**e**) **[P_{66614}][Glu]/[N_{1444}][NTf_2]** at 28.8 °C on cooling; (**f**) **[P_{66614}][Glu]/[N_{2224}][NTf_2]** at 23.1 °C on heating; (**g**) **[P_{66614}][Glu]/[C_1C_4pip][NTf_2]** at 21.3 °C on heating; (**h**) **[P_{66614}][Glu]/[C_1C_4pyrr][NTf_2]** at 21.3 °C on heating.

Images in Figure 3 point out the relevance of gelator nature in affecting gel morphology. Indeed, ammonium salt gives more compact texture than phosphonium ones, as accounted for by the comparison among POM images recorded for **[N_{4444}][Glu]/[N_{1444}][NTf_2]**, **[P_{4444}][Glu]/[N_{1444}][NTf_2]** and **[P_{66614}][Glu]/[N_{1444}][NTf_2]** (Figures 3a, c and e). Surprisingly, cooling of **[N_{4444}][Glu]/[N_{1444}][NTf_2]** allowed observing the presence of strongly coloured crystallites already at 35.7 °C (Figure 3b).

View Article Online
DOI: 10.1039/C8GC01615A

On going from ammonium to phosphonium gelators, morphology changed from a thick to fibrous texture. The presence of fibers just sketched for **[P4 4 4 4][Glu]** – based ILGs, appeared clearly visible in the case of **[P6 6 6 14][Glu]** (Figures 3c, e).

The different nature of ILs also affects ILGs network organisation. Both in the case of **[P4 4 4 4][Glu]** and **[P6 6 6 14][Glu]**, a transition from a fibrous to a thick texture was detected on going from a more to a less viscous IL (**[N1 4 4 4][NTf2]** and **[N2 2 2 4][NTf2]**) (Figures 3c-d and 3e-f).

Finally, morphology also changed on going from acyclic to cyclic ammonium cation of IL, as accounted for by the comparison among POM images collected for **[P6 6 6 14][Glu]** in different ILs. Indeed, the presence of piperidinium or pyrrolidinium cation in the solvent, clearly favoured the occurrence of a mixed network featured by the presence of both fibrous and spherulitic motifs (Figures 3g-h). The latter ones appeared predominant for **[P6 6 6 14][Glu]/[C1C4pyrr][NTf2]**.

Self-repairing ability. ILGs phases were also tested for their self-repairing ability, *i. e.* the ability to repair after the action of external stimuli. In particular, we took in consideration their ability to respond to the action of magnetic stirring or ultrasound irradiation, in order to assess their thixotropic or sonotropic behaviour, respectively.

Thixotropic behaviour has been largely investigated in the case of both organo- and hydrogels.[49, 50] Sonotropy has been much less investigated.[15, 51, 52] However, both abilities were recently reported for ILGs.[29, 31, 32, 34] Our data are displayed in Table 3.

Table 3. Thixotropic and sonotropic behaviour of ionogels at 6.5% wt.

IL	Gelator	Thixotropic	Sonotropic
[N2 2 2 4][NTf2]	**[P6 6 6 14][Glu]**	Yes	Stable*
	[P4 4 4 4][Glu]	Yes	No
[N1 4 4 4][NTf2]	**[P6 6 6 14][Glu]**	Yes	Yes
	[P4 4 4 4][Glu]	No	Yes
	[N4 4 4 4][Glu]	Yes	Yes
[C1C4pip][NTf2]	**[P6 6 6 14][Glu]**	Yes	Yes
[C1C4pyrr][NTf2]	**[P6 6 6 14][Glu]**	Yes	Stable*

*= after 5 min of sonication, the gel phase persists.

As far as thixotropic behaviour is concerned, with the only exception of **[P4 4 4 4][Glu]/[N1 4 4 4][NTf2]**, all gel phases proved to be able to positively respond to the action of mechanical stimulus. In contrast, for the sonotropic behaviour, we obtained different results. Indeed, in the case of **[P6 6 6 14][Glu]/[N2 2 2 4][NTf2]** and **[P6 6 6 14][Glu]/[C1C4pyrr][NTf2]**, gel phases were stable to ultrasound irradiation. Conversely, **[P4 4 4 4][Glu]/[N2 2 2 4][NTf2]** didn't show sonotropic behaviour.

Interestingly, soft materials formed after mechanical or sonochemical disruption exhibited reproducible T_{gel}, allowing us to state once more their reversibility.

Rheology measurements. Mechanical properties of ILGs were analysed performing strain sweep measurements at 1Hz frequency (Figure 4 and S4).

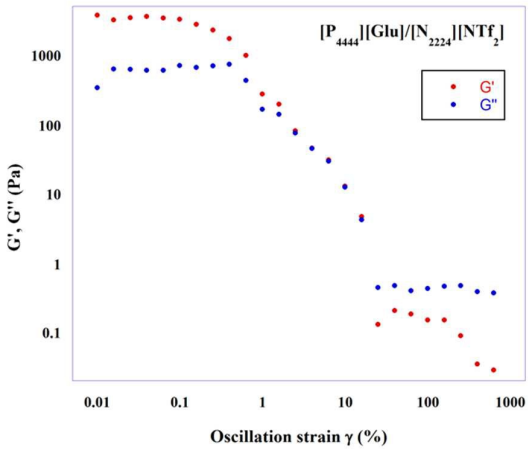

Figure 4. Strain sweep measurement at f = 1Hz for **[P4 4 4 4][Glu]/[N2 2 2 4][NTf2]** at 6.5 wt %.

However, in some cases, namely for **[P6 6 6 14][Glu]/[N2 2 2 4][NTf2]**, **[P6 6 6 14][Glu]/[C1C4pyrr][NTf2]** and **[P6 6 6 14][Glu]/[C1C4pip][NTf2]**, we were unable to perform rheology measurements because the gels were too soft and were disintegrated before obtaining reliable data.

In all strain sweep, G' was higher than G'' at low values of strain, indicating a solid-like behaviour, and G' < G'' at higher strains, indicating liquid-like behaviour. These observations support the gel nature of our samples.[53]

To have a measure of the gel strength, we determined the crossover point of yield strain (γ; *i. e.* where G'' becomes equal to G') that represents the level of stress needed to detect the flow of materials. In general, the increase in gel strength induces a corresponding increase in γ values (Table 4).

Table 4. Yield strain (γ) values determined at 1Hz frequency and 25 °C for ILGs at 6.5 wt%. Error limits are based on an average of three different measurements.

Ionogel	Yield Strain γ (%)
[N4 4 4 4][Glu]/[N1 4 4 4][NTf2]	0.40 ± 0.01
[P4 4 4 4][Glu]/[N1 4 4 4][NTf2]	0.37 ± 0.02
[P6 6 6 14][Glu]/[N1 4 4 4][NTf2]	25.28 ± 0.1
[P4 4 4 4][Glu]/[N2 2 2 4][NTf2]	2.46 ± 0.01

View Article Online
DOI: 10.1039/C8GC01615A

Analysis of data collected allows drawing some conclusions about the effect of gelator and IL structure on mechanical properties of gel phases. Indeed, gel phases obtained in $[N_{1444}][NTf_2]$, γ increases along the order: $[N_{4444}][Glu]$ ~ $[P_{4444}][Glu]$ << $[P_{666\,14}][Glu]$, evidencing a scarce relevance of the nature of the cation (ammonium or phosphonium). Differently, for phosphonium ILGs, a significant effect was detected as far as the elongation of the alkyl chain on the cation was taken into consideration. The observed trend reverses the one we detected for the size of the aggregates (see later) and indicates that ILGs with better mechanical response were obtained, maybe due to the presence of smaller aggregates.

On the other hand, as for **$[P_{4444}][Glu]$**, γ increases on going from **$[N_{1444}][NTf_2]$** to **$[N_{2224}][NTf_2]$**. Once again, ILG showing better resistance to flow is characterised by the presence of smaller aggregates (see later). Furthermore, in this case, the different mechanical responses of ILGs seem also to comply with the marked differences detected in morphology of gelatinous networks (spherulitic for **$[P_{4444}][Glu]/[N_{1444}][NTf_2]$** and thick texture for **$[P_{4444}][Glu]/[N_{2224}][NTf_2]$**).

Opacity and RLS measurements. ILGs formation was investigated using opacity and RLS measurements at 20 °C. Opacity, which is measured by the means of UV-vis spectroscopy, gives information about crystallinity of soft materials, reading the absorbance values at 568 nm.[54] Differently, RLS is a special elastic scattering that originates from fluctuation of the solution refractive index.[55, 56] It allows determining the presence of aggregates in solution and gives insights about their size. Indeed, other factors being constant, RLS intensity (I_{RLS}) is directly proportional to the square of molecular volume of aggregates.[57, 58]

The kinetics of the gelatinous network formation (t_g) was determined using both opacity and RLS measurements. Plots of absorbance and I_{RLS} values as a function of time are reported in Figure 5 and S5.

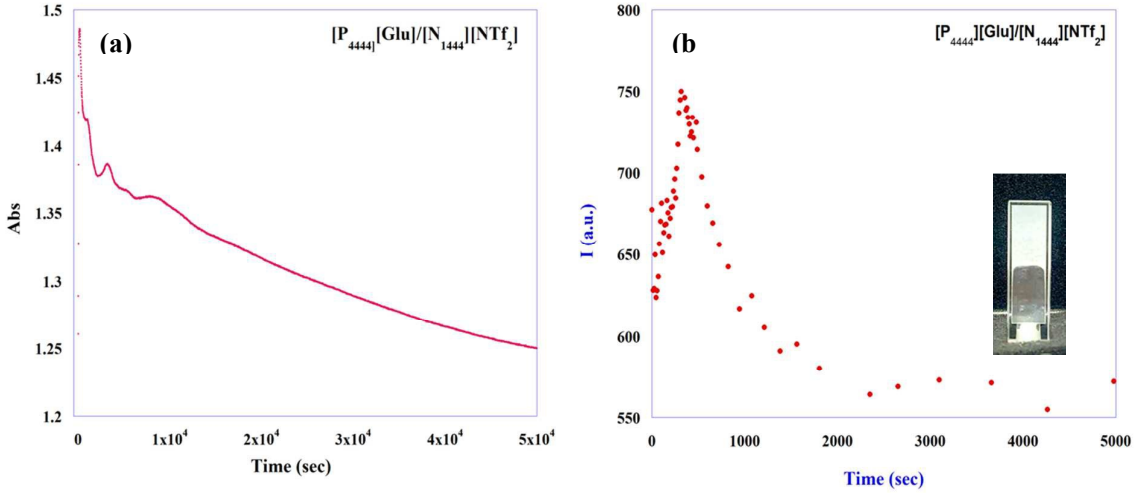

Figure 5. Plots of (**a**) absorbance at 568 nm; (**b**) I_{RLS} as a function of time for **$[P_{4444}][Glu]/[N_{1444}][NTf_2]$**, at 20 °C and 6.5% wt of gelator.

In most cases, we detected the gel phase formation in the quartz cuvette, as assessed by the tube inversion test (Figure 4b).[46, 47] Only for **$[P_{666\,14}][Glu]/[N_{2224}][NTf_2]$** and **$[P_{666\,14}][Glu]/[C_1C_4pyrr][NTf_2]$**, gel phase formation at 20 °C was too slow to perform a kinetic investigation.

Analysis of RLS plots evidences that in some cases: (**$[P_{4444}][Glu]/[N_{1444}][NTf_2]$**, **$[P_{666\,14}][Glu]/[N_{2224}][NTf_2]$**, **$[P_{666\,14}][Glu]/[C_1C_4pip][NTf_2]$**), gelation process occurs *via* a two-step mechanism. We firstly observed a sudden I_{RLS} increase until reaching a maximum value, after which its gradual decrease was detected to reach a constant value (I_g).

To compare different gel phases and analyse the effect of both gelator and IL structural features on the gelation process, we paid attention to gelation time (t_g), corresponding RLS value (I_{RLS}) and opacity (A_g) (Table 5).

View Article Online
DOI: 10.1039/C8GC01615A

Table 5. Gelation time (t_g), RLS intensity (I_{RLS}) and opacity (A_g) of ionogels

Ionogel	I_{RLS} / a. u.	t_g /s	A_g at 568 nm
$[P_{4444}][Glu]/[N_{2224}][NTf_2]$	400	2000	0.8
$[P_{66614}][Glu]/[N_{1444}][NTf_2]$	370	1900	1.15
$[P_{4444}][Glu]/[N_{1444}][NTf_2]$	580	1500	1.3
$[N_{4444}][Glu]/[N_{1444}][NTf_2]$	470	3800	1.5
$[P_{66614}][Glu]/[C_1C_4pip][NTf_2]$	420	1400	1.3

The comparison between data collected for **$[N_{4444}][Glu]$** and **$[P_{4444}][Glu]$** in **$[N_{1444}][NTf_2]$** accounts for a decrease in the size of the aggregates on going from phosphonium to ammonium salts.

Interestingly, the IL nature also plays a role. Indeed, the data pertaining to phosphonium salts indicate that the occurrence of a more organised structure is favoured by an increase in solvent viscosity (moving from **$[N_{2224}][NTf_2]$** to **$[N_{1444}][NTf_2]$**, η = 104.1 and 538.9 cP, respectively)[59, 60] and in the organisation of the cation structure (on going from **$[N_{1444}][NTf_2]$** to **$[C_1C_4pip][NTf_2]$**). Same trend is observed for the opacity measurements with less pronounced differences.

As for the gelation time (t_g), the data collected shed light both on the role played by the gelator and IL nature. In general, gel formation occurs faster for the phosphonium compared to the ammonium salts. Taking into consideration the phosphonium salts, the lengthening of the alkyl chain, on going from **$[P_{4444}][Glu]$** to **$[P_{66614}][Glu]$**, slows down the process. Probably, this is a consequence of the higher conformational freedom of the alkyl chain that makes more difficult the organisation of the 3D network. On the other hand, the IL nature also plays a role in determining the rate of gel phase formation, as accounted for by the significant drop in t_g on going from **$[P_{4444}][Glu]/[N_{2224}][NTf_2]$** to **$[P_{4444}][Glu]/[N_{1444}][NTf_2]$** and the one observed comparing the data relevant to **$[P_{66614}][Glu]/[N_{1444}][NTf_2]$** and **$[P_{66614}][Glu]/[C_1C_4pip][NTf_2]$**.

^{1}H NMR spectroscopy measurements. To have better insights on the driving forces for the self-assembly of our gelators in ILs, we performed a ^{1}H NMR investigation at variable temperatures. In this case, to have detectable signals, we used a gelator concentration much higher than the CGC (12% wt.) and a temperature range between 293 and 373 K.

NMR spectroscopy has been widely used to characterise gel phases as it represents a valuable method to understand how gelators assemble to give fibrillar architectures.[61, 62] In general, as a consequence of reduced transversal relaxation time of aggregates featuring gel phase, gelator peaks are often broadened and hidden under the baseline. Additionally, breakdown of gel network, as a consequence of a concentration decrease or raise in temperature, makes visible the above signals and also induces a chemical shift variation. In particular, temperature changes provide information about the supramolecular forces involved in the aggregation and nanoscale assembly.[63]

In Figures 6 and S6, ^{1}H NMR spectra as a function of temperature, for all gel phases, are reported.

A first look at the spectra evidences how main resonances can be ascribed to the protons of the IL used as a solvent (Figure S6). Obviously, a temperature increase induces a corresponding increase in the resolution of signals without affecting chemical shift values. However, a deep examination of the region between 4.4 and 2.7 ppm allows detection of the presence of some resonances that, as the temperature increases, become more resolved and also show pronounced changes in chemical shift.

View Article Online
DOI: 10.1039/C8GC01615A

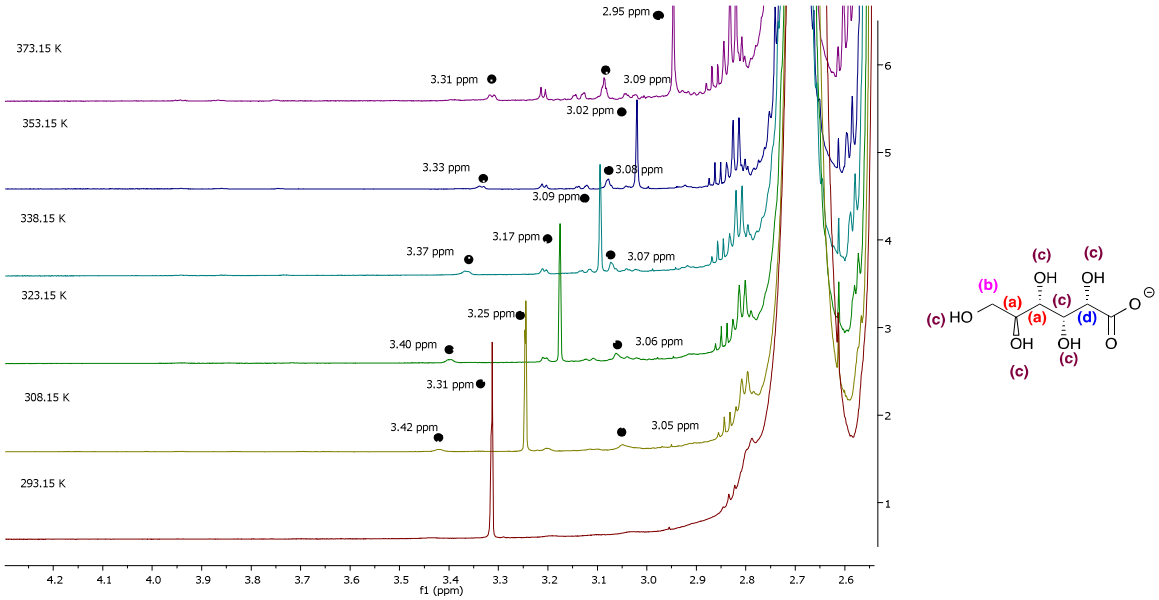

Figure 6. (**a**) Enlarged region of ^{1}H NMR spectra of **[P$_{4\,4\,4\,4}$][Glu]/[N$_{2\,2\,2\,4}$][NTf$_2$]** at 12% wt of gelator as a function of temperature (magenta marker for H_b; brown marker for H_c, red marker for H_a and blue marker for H_d). (**b**) Anion structure with labeled protons. The larger peaks on the extreme right are due to the alkyl chains of **[N$_{2\,2\,2\,4}$][NTf$_2$]**

To identify the above resonances, we recorded ^{1}H NMR spectrum of a dilute solution of **[P$_{4\,4\,4\,4}$][Glu]/[N$_{1\,4\,4\,4}$][NTf$_2$]** in the same temperature range (3% wt; Figure S7). Obviously, the use of gelator concentration lower than CGC prevents gel phase formation, even though the presence of aggregates could not be ruled out.

Analysis of the above spectra evidences how also, in this case, signal resolution increases with a raise in temperature. In particular, the spectrum obtained at 338 K shows a signal at 3.51 ppm, which is assigned to H_b protons, whereas the signal at 3.31 ppm - to H_c protons and the signal at 3.16 ppm - to H_d protons. Integration of these signals is consistent with this assignment.

In particular, H_b and H_d exhibited downfield shift; whereas H_c showed upfield shift. In all cases, the highest chemical shift changes were detected for H_c. According to previous reports,[64] the last upfield shift, as a consequence of gel melting, accounts for the involvement of hydroxyl groups in hydrogen bond formation in the gel network.

With the only exception of **[N$_{4\,4\,4\,4}$][Glu]/[N$_{1\,4\,4\,4}$][NTf$_2$]**, the above changes were linearly correlated with temperature (Figure S8). In the above case, we observed an upfield shift until 338 K. Chemical shift stayed constant above this temperature.

Linear regression analysis was performed according to Equation (1):

$$\delta H_c = m_1 \times T + m_2 \qquad \text{eq.(1)}$$

where m_1 and m_2 represent the intercept and slope of the linear correlation. In particular, the absolute values of slope can be considered as a measure of how easily supramolecular interactions can be broken in the gel network. Higher values should account for a weaker fibrillar network. These values are reported in Table 6.

Table 6. Correlation parameters corresponding to chemical shift variation as a function of temperature for the *H*c of the gluconate anion, according to Equation (1), where *R* = correlation coefficient.

Ionogel	$10^3 \cdot (m_1 \pm \delta m_1)$	$m_2 \pm \delta m_2$	*R*
[P$_{6\,6\,6\,14}$][Glu]/[N$_{1\,4\,4\,4}$][NTf$_2$]	-4.56 ± 0.30	4.64 ± 0.09	0.991
[P$_{6\,6\,6\,14}$][Glu]/[N$_{2\,2\,2\,4}$][NTf$_2$]	-1.12 ± 0.12	3.78 ± 0.04	0.982
[P$_{6\,6\,6\,14}$][Glu]/[C$_1$C$_4$pyrr][NTf$_2$]	-5.33 ± 0.40	4.84 ± 0.12	0.992
[P$_{6\,6\,6\,14}$][Glu]/[C$_1$C$_4$pip][NTf$_2$]	-4.43 ± 0.32	4.56 ± 0.10	0.989
[P$_{4\,4\,4\,4}$][Glu]/[N$_{1\,4\,4\,4}$][NTf$_2$]	-4.75 ± 0.12	4.71 ± 0.04	0.999
[P$_{4\,4\,4\,4}$][Glu]/[N$_{2\,2\,2\,4}$][NTf$_2$]	-6.01 ± 0.58	5.09 ± 0.19	0.982

View Article Online
DOI: 10.1039/C8GC01615A

Journal Name

ARTICLE

On the grounds of the above considerations, **[P$_{6\,6\,6\,14}$][Glu]/[N$_{2\,2\,2\,4}$][NTf$_2$]** should be featured by the strongest interactions and the above result perfectly agrees with the highest $T_{gel\text{-}6.5\%wt}$ measured for the above gel phase. Analysis of slope of these graphs indicates the strength of the supramolecular forces operating in the gel phase. It is affected by the structure of IL cation (data collected for **[P$_{6\,6\,6\,14}$][Glu]**), with significant changes detected both as a function of its geometry ([C$_1$C$_4$pyrr]$^+$ and [C$_1$C$_4$pip]$^+$) and of the alkyl chain on the nitrogen ([**N$_{1\,4\,4\,4}$**]$^+$ and [**N$_{2\,2\,2\,4}$**]$^+$). According to previous reports,[65, 66] the above trend can be ascribed to changes in viscosity of ILs used (η = 84.33 and 255 cP for [C$_1$C$_4$pyrr][NTf$_2$] and [C$_1$C$_4$pip][NTf$_2$], respectively; η = 104.1 and 538.9 cP, for [N$_{2\,2\,2\,4}$][NTf$_2$] and [N$_{1\,4\,4\,4}$][NTf$_2$], respectively).[59, 60, 67]

Furthermore, analysis of the data collected for phosphonium gelators indicates that changes in the gelator structure significantly affect the strength of the interactions operating in the gel network only in less viscous solvents. Indeed, on going from **[P$_{4\,4\,4\,4}$][Glu]** to **[P$_{6\,6\,6\,14}$][Glu]**, significant differences in slope values were detected only for [N$_{2\,2\,2\,4}$][NTf$_2$] ionogels. In the above cases, the presence of longer alkyl chains in **[P$_{6\,6\,6\,14}$][Glu]**, induces a strengthening of the gel network probably due to the increase in van der Waals interactions.

FT-IR measurements. ILGs were also analysed performing FT-IR studies. In particular, this technique has been used to probe hydrogen bond interactions between the molecular building blocks, proving to be useful when –CO, -NH and –OH groups feature the gelator.[68, 69] Figures 7 and S8 display FT-IR spectra for gelators, ILs and ILGs.

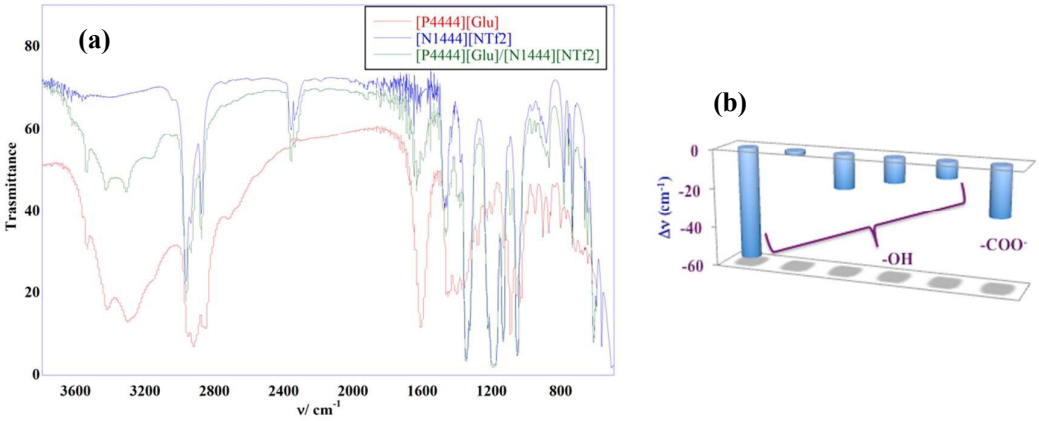

Figure 7. (**a**) FT-IR spectra for neat **[P$_{4\,4\,4\,4}$][Glu]**, **[N$_{1\,4\,4\,4}$][NTf$_2$]** and **[P$_{4\,4\,4\,4}$][Glu]/[N$_{1\,4\,4\,4}$][NTf$_2$]** ILG at 6.5 % wt. (**b**) Changes in stretching frequencies ($\Delta\nu$) on going from gelator to gel phase.

In general, we considered the range 3550-3150 cm^{-1} (OH stretching) and at ~ 1650 cm^{-1} and 1400 cm^{-1} (COO$^-$ stretching) in order to avoid interfering IL absorption bands. In all cases, changes observed in frequencies of hydroxyl and carboxyl groups were significant and according to data collected by using NMR investigation; this points out the relevance of hydrogen bond in favouring the formation of gel network.
Interestingly, shifts detected were affected by gelator nature. Indeed, the highest changes were observed for **[P$_{4\,4\,4\,4}$][Glu]** and the lowest for **[P$_{6\,6\,6\,14}$][Glu]** (Figure S9 and Table S2).
Furthermore, in the case of **[P$_{4\,4\,4\,4}$][Glu]** and **[N$_{4444}$][Glu],** the highest changes in $\Delta\nu$ were detected for hydroxyl group stretching. On the contrary, in the case of **[P$_{66614}$][Glu],** more significant variations were measured for carboxyl group stretching.

Use of ILGs for the desulfurisation of fuels. In this respect, hexane was chosen as the model fuel substitute. As contaminants, thiophene (**T**), benzothiophene (**BT**) and dibenzothiophene (**DBT**) were selected. Standard solutions of **T**, **BT** and **DBT** in hexane were prepared (500 μL) and put in contact with gel phases (250 mg) at 6.5% wt of gelator. In particular, we used only gels formed by **[N$_{4\,4\,4\,4}$][Glu]** and **[P$_{4\,4\,4\,4}$][Glu]**. Due to high solubility of **[P$_{6\,6\,6\,14}$][Glu]** in hexane, it was deemed unsuitable. ILGs used were stable in contact with the hexane solution with no contamination of hexane by ILGs, as accounted for by both HPLC and ^{1}H NMR spectroscopy

View Article Online
DOI: 10.1039/C8GC01615A

(Figure S10). Indeed, in both cases we didn't observe signals corresponding to ILG components. Furthermore, after the complete removal of hexane phase, we didn't determine significant changes in the ILGs weight.

Initially, to evaluate the adsorption ability of our soft materials, contact times of 24 and 48 h were used and the adsorption efficiency (AE) was determined using Equation (2):

$$AE = (C_0\text{-}C_f)/C_0 \qquad \text{eq.(2)}$$

where C_0 and C_f represent the concentration of the sulfur compound before and after the contact with the gel phase, respectively. To compare, the above tests were also performed using pure ILs (Figure 8 and Table S3).

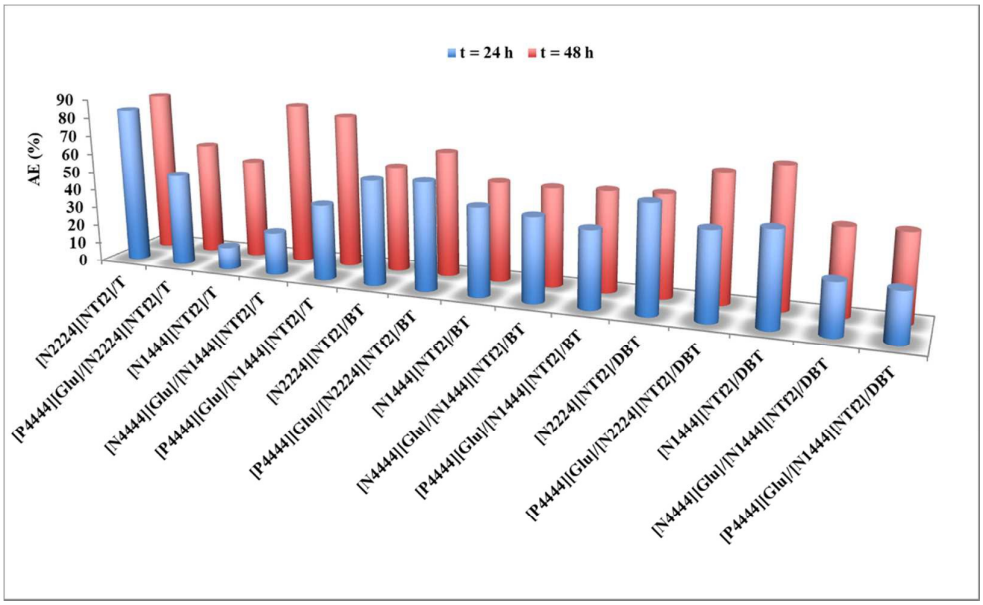

Figure 8. Adsorption efficiency (AE) of sulfur compounds on ILGs [6.5% wt of gelator] and corresponding ionic liquid solvents (in ILGs) at 20 °C. **Blue** columns = 24h; **red** columns= 48h

Analysis of the data collected for ILs gives different trends as a function of solvent nature. AE stayed constant in the case of **$[N_{2224}][NTf_2]$**, whereas it significantly increased on going from 24 up to 48 h for **$[N_{1444}][NTf_2]$**. Furthermore, two different scenarios can exist depending on the nature of the substrate. Taking into consideration values collected at 24 h, AE for **T** significantly increased on going from **$[N_{1444}][NTf_2]$** to **$[N_{2224}][NTf_2]$**. This is in parallel with the IL viscosity drop, according to a previous report that indicates the above parameter as the key factor in desulfurisation of fuels by ILs.[70] In the case of **BT** and **DBT,** less pronounced differences were detected.

A decrease in AE, at 24 h, was detected on going from ILs to the corresponding ILGs for **$[P_{4444}][Glu]/[N_{2224}][NTf_2]/T$**, **$[N_{4444}][Glu]/[N_{1444}][NTf_2]/DBT$** and **$[P_{4444}][Glu]/[N_{1444}][NTf_2]/DBT$** systems (Figure 8). In all other cases, the above parameter stayed constant or increased. At longer times (48 h), in most cases, performance of ILGs resulted comparable or better than the ones of ILs, evidencing the positive role exerted by the presence of the phosphonium or ammonium gelators in the mixture. The above results agree with the good efficiency of phosphonium ILs in performing extractive desulfurisation of fuels recently assessed by Zolfigol and coworkers[37, 71].

These preliminary tests clearly indicate the ability of our systems to act as sorbent systems in desulfurisation of fuels, showing good performance also towards sulfur compounds like **BT** and **DBT**. This represents the first advantage with respect to the adsorption systems so far reported.[2, 72] Indeed, the above compounds are widely known as refractory to the removal by adsorption and this is one of the reasons why this methodology has been partially used previously in desulfurisation of fuels.[21]

Encouraged by the above results, we firstly analysed the temperature effect. To examine this, **$[P_{4444}][Glu]/[N_{2224}][NTf_2]/T$** and **$[P_{4444}][Glu]/[N_{1444}][NTf_2]/T$** systems were considered and adsorption tests at 30 °C for 24 h (Table S3) were performed. The AE value stayed constant in the first case, while in the second case, it was higher than the corresponding one at 20 °C and 24 h. However, if we consider a longer contact time (48 h), raising the temperature results in a lower AE. Previous reports evidence that the temperature barely affects the extraction ability of ILs.[73] This information, together with results

View Article Online
DOI: 10.1039/C8GC01615A

collected, induces us to carry out investigation at 20 °C, also to limit the energy demand of the process.

The next evaluation was the determination of the optimum time needed to obtain the highest AE value for **[P$_{4444}$][Glu]/[N$_{2224}$][NTf$_2$]** and **[P$_{4444}$][Glu]/[N$_{1444}$][NTf$_2$]** ILGs (Figure 9 and Tables S4-S5). These systems were chosen as model ILGs to study the performance of our soft materials. Indeed, both systems showed a similar behaviour as far as **T** is concerned, but very different efficiencies for **BT** and **DBT**.

As far as **[P$_{4444}$][Glu]/[N$_{2224}$][NTf$_2$]** IGL system is concerned, plot of AE as a function of time sheds light on the better efficiency of this system in adsorbing **T** from hexane solution compared to **BT** and **DBT** (Figure 9a).

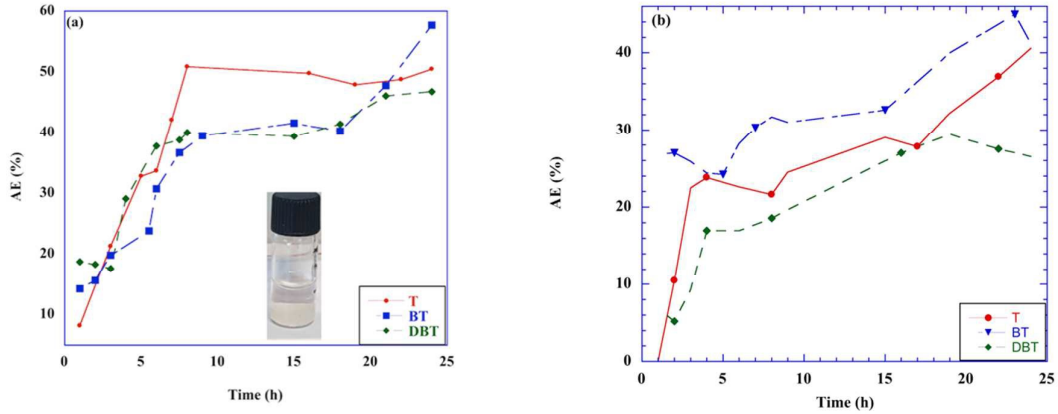

Figure 9. Plots of AE of sulfur compounds as a function of time for (**a**) **[P$_{4444}$][Glu]/[N$_{2224}$][NTf$_2$]** (Inset: picture of the adsorption system) and (**b**) **[P$_{4444}$][Glu]/[N$_{1444}$][NTf$_2$]** at 20 °C and at 6.5% wt of gelator.

On the contrary, in the case of **[P$_{4444}$][Glu]/[N$_{1444}$][NTf$_2$]**, smaller differences were detected as a function of time (Figure 9b). The compatibility between our gels and sulfur compounds is structure dependent. Therefore, the above differences can be ascribed to diversity in porosity of ILGs, as a consequence of the different organization of gel networks. On this subject, it is well known that supramolecular gels are able to perform molecular recognition[74] and this should explain why extraction time differently affects the adsorption of sulfur compounds.

In general, the comparison among the AEs detected for two ILGs evidences better performance for **[P$_{4444}$][Glu]/[N$_{2224}$][NTf$_2$]**, probably as a consequence of the lower viscosity of the IL used as solvent.

After 7h of contact, all systems gave the highest AE. Consequently, we used this contact time to study a more realistic situation, taking into consideration mixtures of three sulfur compounds (Tables S6).

In general, AE measured for a total sulfur concentration of 1500 ppm**,** was surprisingly higher for the mixture of contaminants in comparison to individual component solutions (Figure 10 and Table S6), evidencing that the simultaneous presence of aromatic hydrocarbons exerts a synergetic effect on the adsorption process.

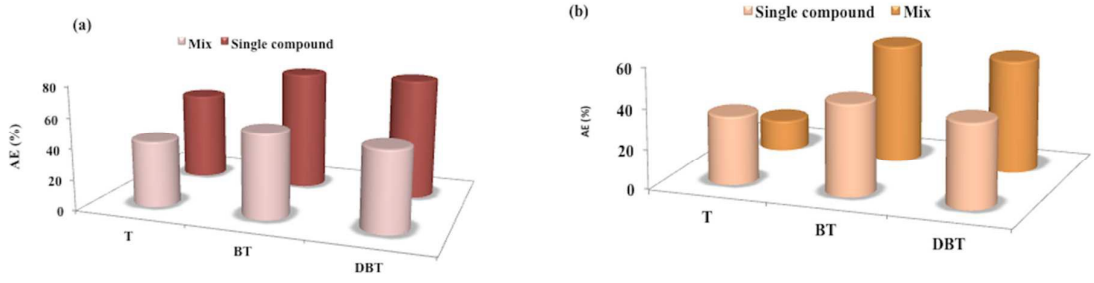

Figure 10. Comparison of AE, determined at 20 °C, for solution of single compounds and mixed solutions of sulfur compounds (C = 1500 ppm) corresponding to **(a) [P$_{4444}$][Glu]/[N$_{2224}$][NTf$_2$]** and **(b) [P$_{4444}$][Glu]/[N$_{1444}$][NTf$_2$]** at 6.5% wt of gelator.

View Article Online
DOI: 10.1039/C8GC01615A

Journal Name

ARTICLE

At present, the exact nature of this synergetic effect is not well understood. Interestingly, the most relevant effect was detected in the case of **BT** and **DBT** that generally show high resistance towards removal by both extractive and oxidative methods.[21] Furthermore, as real fuels might also contain a fraction of aromatics, we tested the stability of ILGs to the contact with benzene solution in hexane at different concentrations (500 and 2000 ppm). Once again, we didn't observe contamination of fuel by the ILG components (Figure S11).

To further deepen the knowledge of the systems used, we also analysed key parameters determining the outcome of adsorption processes, such as concentration of the sulfur compounds in the fuel and its volume. We changed the concentration from 900 to 3000 ppm (Table S8). The data collected show that, both ILGs had better performance when they acted on more concentrated solutions. Indeed, in all cases, AE increased in parallel with concentration. Interestingly, the concentration effect depends on the gel nature, as accounted for more drastic changes in AE detected in the case of **$[P_{4\,4\,4\,4}][Glu]/[N_{1\,4\,4\,4}][NTf_2]$** compared to **$[P_{4\,4\,4\,4}][Glu]/[N_{2\,2\,2\,4}][NTf_2]$.**

As stated above, among the factors analysed, we also took into consideration the effect of a different fuel volume. For this, using 250 mg of gel phase and mixed solutions at 1500 ppm, we changed the volume from 300 μL up to 700 μL (Table S8). Interestingly, we observed that our gel phases stayed stable even after doubling the volume. However, in the analysed range, the volume of fuel did not affect the performance of gel phases. AE values stayed constant or showed small changes on going from 300 up to 500 μL. A decrease in the above parameter was detected only using 700 μL of fuel.

From the operational point of view, another important factor may be the contact surface area between fuel and gel phase. For this, bearing in mind that our gel phases could be used as stationary phases of columns, we changed the diameter of the vial keeping constant the ratio between the volume of the fuel and the mass of the gel phase [V_{fuel} (μL)/m_{gel} (mg)= 2; Table S9]. For both systems, we observed a decrease in AE with the increase in the contact surface area that was more significant in the case of **$[P_{4\,4\,4\,4}][Glu]/[N_{2\,2\,2\,4}][NTf_2]$** compared to **$[P_{4\,4\,4\,4}][Glu]/[N_{1\,4\,4\,4}][NTf_2]$**, indicating that sorbents studied probably will work better in longer than in broader columns.

Finally, we assessed the possibility of reusing our adsorption systems. After removal of the fuel, we verified the gel nature of our samples by the tube inversion test[46, 47] and we put in contact the sulfur compounds laden gel with a fresh portion of the fuel. We tried to reuse the ILGs 3-4 times and, in the above conditions, **$[P_{4\,4\,4\,4}][Glu]/[N_{2\,2\,2\,4}][NTf_2]$** and **$[P_{4\,4\,4\,4}][Glu]/[N_{1\,4\,4\,4}][NTf_2]$** retained 40% of their adsorption ability (Figure 11 and Table S10).

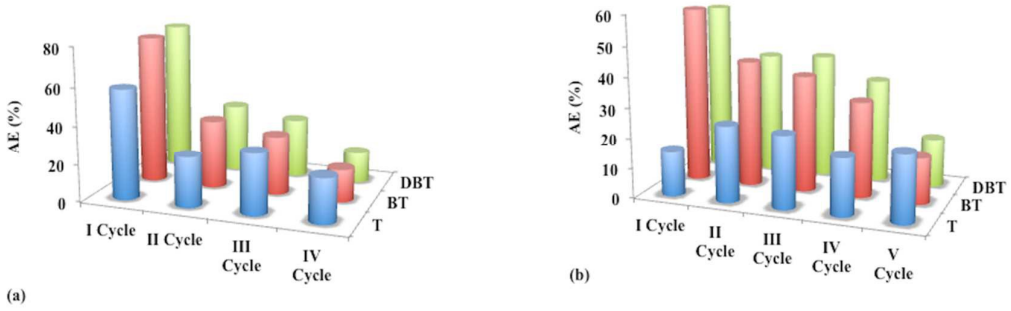

Figure 11. Cycles of reusing performed at 20 °C (C = 1500 ppm) corresponding to **(a) $[P_{4\,4\,4\,4}][Glu]/[N_{2\,2\,2\,4}][NTf_2]$** and **(b) $[P_{4\,4\,4\,4}][Glu]/[N_{1\,4\,4\,4}][NTf_2]$** at 6.5% wt of gelator.

Here, a comparison with other sorbent systems previously reported in literature is mandatory. Unfortunately, the lack of data concerning the use of supramolecular gels as sorbent systems for desulfurisation of fuels does not allow the direct comparison. Notwithstanding the above premises, some relevant examples of adsorption systems recently published are reported in Table 7.[75-81] Obviously, the proposed list is limited, also because a comprehensive review of data previously reported is out of our scope.

View Article Online
DOI: 10.1039/C8GC01615A

Table 7. AE (%) for sorbent systems previously reported in literature.

Sorbent System	AE (%)
Metal nanoparticles on activated carbon[77]	**T**: 10-50
	BT: 10-50
	DBT: 70-90
NaY and NiY Zeolites[75]	**BT**: 59 and 75
Bamboo-derived biochairs[80]	**BT**: 60
Acid treated activated charcoal[78]	**DBT**: 90
Molybdenum containing ordered mesoporous silica[81]	**BT** and **DBT**: 90
$[P_{4\,4\,4\,4}][Glu]$/$[N_{2\,2\,2\,4}][NTF_2]$[a]	**T**: 60
	BT and **DBT**: 80
$[mim(CH_2)_4SO_3H][Tos]$[76]	**T:** 38
	BT: 50 and **DBT:** 52
$[C_4mim][SCN]$[79]	**DBT:** 66.1
$[N_{1\,4\,4\,4}][CH_3SO_3]$[79]	**DBT:** 61.9
$[C_6mim][BF_4]$[79]	**DBT:** 53.5
$[C_1C_4pyrr][NTf_2]$[82]	**T:** 40
	BT: 40
	DBT: 47
$[C_1C_4pip][NTf_2]$[83]	**T:** 60
	BT: 64
	DBT: 58

[a]This work; AE values were reproducible within ± 2 %.

In general, proposed systems work in a contact time ranging from 5 min up to 6 h and in temperature range 25-35 °C. The data reported in Table 7 are well in line with the ones previously reported in literature and in some cases, they also prove more efficient than single ionic liquid systems. Moreover, our system is devoid of any heavy metals.

The advantage of using ILGs compared to simple ILs is that in most cases, **AE** values prove comparable or better than the ones obtained using ILs as extraction phases. Similarly, to our ILGs, ILs are frequently reused for 3-4 times. However, the self-supporting and highly porous nature of ILGs could allow an easier handling of sorbent systems and a lower loss of cleaning materials compared to liquid-liquid systems, also taking in consideration the very low solubility of ILG components in the fuel.

Conclusions

In order to identify novel materials with green environmentally friendly components in them for desulfurisation of fuels, we explored the possibility of using supramolecular gels as sorbent systems. Conjugating properties of ILs already known as efficient systems in extractive desulfurisation processes, with the ones of gluconate-based ammonium and phosphonium salts, we obtained novel ILGs. Salts used as gelators behave themselves as ILs and are based on a renewable sugar able to give a thick network of hydrogen bonds. To the best of our knowledge, this is the first report that studies such kind of systems in adsorption processes aimed at lowering the level of sulfur compounds in fuels.

Serendipitously, these systems were able to remove about 70-80 % of **BT** and **DBT** that generally are claimed as refractory compounds in desulfurisation. When a mixture of sulfureous contaminants was present in the fuel, a synergetic effect was observed with respect to their removal.

Currently, the exact mechanism of adsorption process is not known. On the grounds of previous reports about the use of glyceryl-functionalised ILs in desulfurisation of fules,[37] we presume a pivotal role played by hydroxyl groups of gluconate anion in interacting with sulfur compounds, favouring their adsorption. However, we reserve a future and detailed investigation on this aspect and also on the complete removal of sulfur compounds from ILGs, possibly utilising catalytic photodegradation[84] or cavitation.[85]

Our approach proves highly versatile, as ILGs are formed by binary mixture of ILs and this paves the way to test a number of combinations.

With all this in mind, our future goal is to use these ILGs in flow systems where the ILGs comprise the stationary phase and then to optimise all structural and operational parameters that would culminate their performance.

Experimental

Materials. D-gluconic acid aqueous solution (49-53 wt. % in H_2O), trihexyltetradecylphosphonium chloride, tetrabutylphosphonium hydroxide solution (40 wt. % in H_2O), tetrabutylammonium hydroxide solution (40 wt. % in H_2O), $[C_1C_4pyrr]Cl$, $[C_1C_4pip]Cl$, $[N_{2\,2\,2\,4}]Cl$, $[N_{1\,4\,4\,4}]Cl$ and

View Article Online
DOI: 10.1039/C8GC01615A

bis{(trifluoromethyl)sulfonyl}amide lithium salt were purchased and used without further purification.

Ethanol, methanol were purchased and used without further purification.

Mass spectrometric measurements. ESMS-mass spectrometric measurements were carried out on a Waters ICI Premier instrument with an Adylon Trìversa NanoMate injection system (cone voltage 50 V, source 120 °C). Both positive and negative ions were detected. For each sample was prepared a solution using methanol as solvent.

Differential scanning calorimetry. DSC measurements were carried out using a Q20 instrument calibrated using indium as standard and TA Instruments Modulated DSC Q 2000 V24.4 Build 116 with a refrigerated cooling system RCS 90 capable of controlling the temperature down to 220 K. Samples were weighed and hermetically sealed in aluminum pans. Heating and cooling rates were 10 °C min^{-1} for the salts samples and 5 °C min^{-1} for the gels experiments. The maximum heating temperature was varied in dependence on the thermal stability of the sample, instead, the minimum cooling temperature was set in dependence on the instrument at -10 °C under nitrogen atmosphere. Two heat-cool cycles were performed for each sample.

Thermogravimetric analysis. Thermogravimetric analysis was performed using TGA/DSC thermogravimetric analyser from Mettler-Toledo, Inc. The samples were measured in alumina crucibles, at a heating rate of 5 K min^{-1} under a nitrogen atmosphere. The onset of the weight loss in each thermogram was used as a measure of the decomposition temperature (point at 5 wt% loss of the sample).

POM measurements. The POM images of the salts and the gel phases were recorded using an Olympus BX50 microscope equipped with JVC TK-1085E camera. For all experiments, the 0.25 10X MD PLAN lens was used. The salts samples were cast between two glasses to record the POM images. In all cases, two consecutive heating-cooling cycles were performed.

The gels phases were not covered with the glass above to not destroy the gel phase. The salts were heated until melting and then cooled. The gels were heated until 90 °C and then cooled. Heating and cooling rates were 5 °C min^{-1}.

Gelation tests. The salt was weighed in a vial and a proper solvent was added, the first concentration considered was 1 wt. % (2.5 mg of salt in 250 mg of solvent). If the salt was insoluble at room temperature, the solution was heated for 1.5h, at a temperature that is ~< 10 °C than the boiling point of the solvent. After the heating, the clear solution was immediately put in the fridge (4 °C) overnight. After this time, if it was still a solution, or it drips with the tube inversion test,[46] the concentration of the salt was increased.

T_{gel} determination. The T_{gel} values were determined with the lead ball method.[48] The lead ball (weighing 46.23 mg and 2 mm in diameter) was placed on top of the gel, and the vial was placed in a water bath. The temperature of the bath was increased of 2 °C/min till the lead ball, going through the gel phase, reached the bottom of the vial (T_{gel}). The T_{gel} values were reproducible within 1 °C.

Opacity measurements. Opacity measurements were recorded with a spectrophotometer (Beckman Coulter DU 800). The limpid hot solution of the salt was put in a quartz cuvette with light path of 0.2 cm. The kinetic of gel formation was recorded at a wavelength of 568 nm and a temperature of 20 °C. Spectra were recorded until gel formation. The gel phase obtained at the end of the measurement was stable after the tube inversion test.[46]

RLS measurements. RLS measurements were carried out at 20 °C on a spectrofluorophotometer (JASCO FP-777W) using a synchronous scanning mode. The RLS spectrum was recorded from 300 to 600 nm with both the excitation and emission slit widths set at 1.5 nm. The maximum intensity of the spectrum obtained was chosen as the working wavelength.

The sample preparation was the same of the opacity measurements, putting the clear hot solution of the salt in the cuvette. The spectra were recorded until constant values of intensity (gel formation). The gel phase obtained at the end of the measurement was stable after the tube inversion test.[46]

NMR measurements. ^{1}H NMR and ^{13}C NMR spectra were recorded using Bruker AV-300, Bruker ultrashield 400 plus, Bruker-spectroscopin 400 ultrashield and nuclear magnetic resonance spectrometers. Chemical shifts were reported relative to $SiMe_4$. The VT ^{1}H NMR were recorded using the Ascend™ 600 Bruker with an internal solvent reference (d_6-DMSO). Each gel was formed inside the NMR tube containing the solvent reference inside. The spectra were recorded from 293 up to 373 K; for each temperature, the sample was equilibrated for 20 min.

Spectra of hexane solution put in contact with gel phases were recorded using A steam coaxial capillary tube loaded with [D6]DMSO was used for the external lock of the NMR spectroscopy magnetic field/frequency and its signal was used as the ^{1}H NMR spectroscopy external reference at δ=2.56 ppm.

Adsorption of sulfur compounds. Each experiment was carried out at 20 °C. The solution, at fixed ppm concentration (500 μL), was put on the top of the gel (250 mg), and after the established time, 200 μL of the solution were used to run the HPLC measurement. The concentration of sulfur compound(s) still present in solution was determined using a previously obtained calibration curve. The adsorption efficiency of sulfur compounds was determined using a HPLC Shimadzu LC-10 AD, equipped with an inverse phase C18 column. Binary mixture ACN/H_2O (80/20; v/v) was used as eluent with a flow of 1 mL min^{-1}.

Conflicts of interest

There are no conflicts to declare.

Acknowledgements

View Article Online
DOI: 10.1039/C8GC01615A

We thank MIUR (FIRB 2010RBFR10BF5V) for financial support. FB and NVP gratefully acknowledge QUILL and its Industrial Advisory Board. Richard Murphy from QUB is thanked for his assistance with recording NMR spectra.
This article is dedicated to the memory of co-author, Prof. Kenneth R. Seddon, who with his enthusiasm and unwavering support moved the whole project.

Notes and references

1. P. Marion, B. Bernela, A. Piccirilli, B. Estrine, N. Patouillard, J. Guilbot and F. Jerome, *Green Chem.*, 2017, **19**, 4973-4989.
2. V. Chandra Srivastava, *RSC Adv.*, 2012, **2**, 759-783.
3. S. A. Dharaskar, K. L. Wasewar, M. N. Varma, D. Z. Shende, K. K. Tadi and C. K. Yoo, *Fuel Process. Technol.*, 2014, **123**, 1-10.
4. Z. Alipoor, A. Behrouzifar, S. Rowshanzamir and M. Bazmi, *Energy Fuels*, 2015, **29**, 3292-3301.
5. D. Boniek, D. Figueiredo, A. F. B. dos Santos and M. A. de Resende Stoianoff, *Clean Technologies and Environmental Policy*, 2015, **17**, 29-37.
6. A. J. Hernández-Maldonado and R. T. Yang, *J. Am. Chem. Soc.*, 2004, **126**, 992-993.
7. H. Mei, B. W. Mei and T. F. Yen, *Fuel*, 2003, **82**, 405-414.
8. Y. N. Prajapati and N. Verma, *Fuel*, 2017, **189**, 186-194.
9. G. Abdi, M. Ashokkumar and A. Alizadeh, *Fuel*, 2017, **210**, 639-645.
10. P. Misra, S. Badoga, A. Chenna, A. K. Dalai and J. Adjaye, *Chem. Eng. J. (Lausanne)*, 2017, **325**, 176-187.
11. J. Wang and J. Wei, *Journal of Materials Chemistry A*, 2017, **5**, 4651-4659.
12. A. A. Iravani, K. Gunda and F. T. T. Ng, *AIChE J.*, 2017, **63**, 5044-5053.
13. Z. Sun, Q. Huang, T. He, Z. Li, Y. Zhang and L. Yi, *ChemPhysChem*, 2014, **15**, 2421-2430.
14. D. B. Amabilino, D. K. Smith and J. W. Steed, *Chem. Soc. Rev.*, 2017, **46**, 2404-2420.
15. C. D. Jones and J. W. Steed, *Chem. Soc. Rev.*, 2016, **45**, 6546-6596.
16. P. C. Marr and A. C. Marr, *Green Chem.*, 2016, **18**, 105-128.
17. H. L. Hwang, S. R. Jadhav, J. R. Silverman and G. John, *J. Chem. Educ.*, 2014, **91**, 1563-1568.
18. G. John, B. Vijai Shankar, S. R. Jadhav and P. K. Vemula, *Langmuir*, 2010, **26**, 17843-17851.
19. B. O. Okesola and D. K. Smith, *Chem. Soc. Rev.*, 2016, **45**, 4226-4251.
20. S. Marullo, C. Rizzo, N. T. Dintcheva, F. Giannici and F. D'Anna, *J. Colloid Interface Sci.*, 2018, **517**, 182-193.
21. M. H. Ibrahim, M. Hayyan, M. A. Hashim and A. Hayyan, *Renewable and Sustainable Energy Reviews*, 2017, **76**, 1534-1549.
22. O. U. Ahmed, F. S. Mjalli, T. Al-Wahaibi, Y. Al-Wahaibi and I. M. AlNashef, *Ind. Eng. Chem. Res.*, 2015, **54**, 6540-6550.
23. O. U. Ahmed, F. S. Mjalli, A.-W. Talal, Y. Al-Wahaibi and I. M. Al Nashef, *J. Solution Chem.*, 2018, **47**, 468-483.
24. S. Dharaskar and M. Sillanpaa, *Chem. Eng. Res. Des.*, 2018, **133**, 388-397.
25. S. Dharaskar, M. Sillanpaa and K. K. Tadi, *Environmental Science and Pollution Research*, 2018, DOI: 10.1007/s11356-018-1789-5.
26. W. Jiang, W. Zhu, H. Li, X. Wang, S. Yin, Y. Chang and H. Li, *Fuel*, 2015, **140**, 590-596.
27. N. F. Nejad, E. Shams, M. Adibi, A. A. Miran Beigi and S. K. Torkestani, *Pet. Sci. Technol.*, 2012, **30**, 1619-1628.
28. F. D'Anna and R. Noto, *Eur. J. Org. Chem.*, 2014, **2014**, 4201-4223.
29. F. D'Anna, C. Rizzo, P. Vitale, G. Lazzara and R. Noto, *Soft Matter*, 2014, **10**, 9281-9292.
30. P. McNeice, Y. Zhao, J. Wang, G. F. Donnelly and P. C. Marr, *Green Chem.*, 2017, **19**, 4690-4697.
31. C. Rizzo, R. Arrigo, N. T. Dintcheva, G. Gallo, F. Giannici, R. Noto, A. Sutera, P. Vitale and F. D'Anna, *Chem. Eur. J.*, 2017, **23**, 16297-16311.
32. C. Rizzo, F. D'Anna, R. Noto, M. Zhang and R. G. Weiss, *Chem. Eur. J.*, 2016, **22**, 11269-11282.
33. I. Dinares, C. Garcia de Miguel, A. Ibanez, N. Mesquida and E. Alcalde, *Green Chem.*, 2009, **11**, 1507-1510.
34. C. Rizzo, F. Arcudi, L. Đorđević, N. T. Dintcheva, R. Noto, F. D'Anna and M. Prato, *ACS Nano*, 2017, DOI: 10.1021/acsnano.7b07529.
35. C. Iacob, J. R. Sangoro, W. K. Kipnusu, R. Valiullin, J. Karger and F. Kremer, *Soft Matter*, 2012, **8**, 289-293.
36. S. J. Craythorne, K. Anderson, F. Lorenzini, C. McCausland, E. F. Smith, P. Licence, A. C. Marr and P. C. Marr, *Chem. Eur. J.*, 2009, **15**, 7094-7100.
37. F. R. Moghadam, S. Azizian, M. Bayat, M. Yarie, E. Kianpour and M. A. Zolfigol, *Fuel*, 2017, **208**, 214-222.
38. Y. Jiang, K. Liu, H. Zhang, Y. Wang, Q. Yuan, N. Su, J. Bao and X. Fang, *ACS Sustainable Chemistry & Engineering*, 2017, **5**, 6116-6123.
39. K. S. Egorova and V. P. Ananikov, *ChemSusChem*, 2014, **7**, 336-360.
40. M. Khaled, *Res. Chem. Intermed.*, 2015, **41**, 9817-9833.
41. S. E. E. Warrag, N. R. Rodriguez, I. M. Nashef, M. van Sint Annaland, J. I. Siepmann, M. C. Kroon and C. J. Peters, *J. Chem. Eng. Data*, 2017, **62**, 2911-2919.
42. C. Guerrero-Sanchez, T. Lara-Ceniceros, E. Jimenez-Regalado, M. Raşa and U. S. Schubert, *Adv. Mater.*, 2007, **19**, 1740-1747.
43. D. F. Martin, M. Shamma and W. C. Fernelius, *J. Am. Chem. Soc.*, 1958, **80**, 4891-4895.
44. K. R. Seddon, A. Stark and M.-J. Torres, *Pure Appl. Chem.*, 2000, **72**, 2275-2287.
45. J. Yang, Q. Zhang, L. Zhu, S. Zhang, J. Li, X. Zhang and Y. Deng, *Chem. Mater.*, 2007, **19**, 2544-2550.
46. S. R. Raghavan and B. H. Cipriano, in *Molecular Gels: Materials with Self-Assembled Fibrillar Networks*, eds. R. G. Weiss and P. Terech, Springer Netherlands, Dordrecht, 2006, DOI: 10.1007/1-4020-3689-2_9, pp. 241-252.
47. S. Raghavan and B. Cipriano, *(Eds.: R. Weiss, P. Terech), Springer, Dordrecht,*

2006, pp. 241–252.
48. A. Takahashi, M. Sakai and T. Kato, *Polym. J. (Tokyo, Jpn.)*, 1980, **12**, 335.
49. V. A. Mallia, M. George, D. L. Blair and R. G. Weiss, *Langmuir*, 2009, **25**, 8615-8625.
50. X. Yu, L. Chen, M. Zhang and T. Yi, *Chem. Soc. Rev.*, 2014, **43**, 5346-5371.
51. S. Baddi, S. S. Madugula, D. S. Sarma, Y. Soujanya and A. Palanisamy, *Langmuir*, 2016, **32**, 889-899.
52. A. Nuthanakanti and S. G. Srivatsan, *Nanoscale*, 2016, **8**, 3607-3619.
53. A. Garai and A. K. Nandi, *Journal of Polymer Science Part B: Polymer Physics*, 2008, **46**, 28-40.
54. P. Terech, D. Pasquier, V. Bordas and C. Rossat, *Langmuir*, 2000, **16**, 4485-4494.
55. W. Lu, B. S. Fernández Band, Y. Yu, Q. Geng Li, J. Chuan Shang, C. Wang, Y. Fang, R. Tian, L. Ping Zhou, L. Li Sun, Y. Tang, S. Hua Jing, W. Huang and J. Ping Zhang, *Microchim. Acta*, 2007, **158**, 29-58.
56. R. F. Pasternack, C. Bustamante, P. J. Collings, A. Giannetto and E. J. Gibbs, *J. Am. Chem. Soc.*, 1993, **115**, 5393-5399.
57. J. Anglister and I. Z. Steinberg, *J. Chem. Phys.*, 1983, **78**, 5358-5368.
58. J. Zheng, X. Wu, M. Wang, D. Ran, W. Xu and J. Yang, *Talanta*, 2008, **74**, 526-532.
59. A. Bhattacharjee, A. Luís, J. H. Santos, J. A. Lopes-da-Silva, M. G. Freire, P. J. Carvalho and J. A. P. Coutinho, *Fluid Phase Equilib.*, 2014, **381**, 36-45.
60. C.-P. Lee, J.-D. Peng, D. Velayutham, J. Chang, P.-W. Chen, V. Suryanarayanan and K.-C. Ho, *Electrochim. Acta*, 2013, **114**, 303-308.
61. B. Escuder, M. Llusar and J. F. Miravet, *J. Org. Chem.*, 2006, **71**, 7747-7752.
62. Y. E. Shapiro, *Prog. Polym. Sci.*, 2011, **36**, 1184-1253.
63. A. R. Hirst, I. A. Coates, T. R. Boucheteau, J. F. Miravet, B. Escuder, V. Castelletto, I. W. Hamley and D. K. Smith, *J. Am. Chem. Soc.*, 2008, **130**, 9113-9121.
64. V. J. Nebot and D. K. Smith, in *Functional Molecular Gels*, The Royal Society of Chemistry, 2014, DOI: 10.1039/9781849737371-00030, pp. 30-66.
65. L. Niu, J. Song, J. Li, N. Tao, M. Lu and K. Fan, *Soft Matter*, 2013, **9**, 7780-7786.
66. H. Xu, J. Song, T. Tian and R. Feng, *Soft Matter*, 2012, **8**, 3478-3486.
67. J. G. Huddleston, A. E. Visser, W. M. Reichert, H. D. Willauer, G. A. Broker and R. D. Rogers, *Green Chem.*, 2001, **3**, 156-164.
68. D. J. Abdallah, L. Lu and R. G. Weiss, *Chem. Mater.*, 1999, **11**, 2907-2911.
69. M. Suzuki, M. Nanbu, M. Yumoto, H. Shirai and K. Hanabusa, *New J. Chem.*, 2005, **29**, 1439-1444.
70. R. Abro, A. A. Abdeltawab, S. S. Al-Deyab, G. Yu, A. B. Qazi, S. Gao and X. Chen, *RSC Adv.*, 2014, **4**, 35302-35317.
71. E. Kianpour, S. Azizian, M. Yarie, M. A. Zolfigol and M. Bayat, *Chem. Eng. J. (Lausanne)*, 2016, **295**, 500-508.
72. I. Ahmed, T. Panja, N. A. Khan, M. Sarker, J.-S. Yu and S. H. Jhung, *ACS Appl. Mater. Interfaces*, 2017, **9**, 10276-10285.
73. F. R. Moghadam, S. Azizian, M. Bayat, M. Yarie, E. Kianpour and M. A. Zolfigol, *Fuel*, 2017, **208**, 214-222.
74. J. A. Saez, B. Escuder and J. F. Miravet, *Chem. Commun.*, 2010, **46**, 7996-7998.
75. V. A. Kusuma, M. K. Macala, J. Liu, A. M. Marti, R. J. Hirsch, L. J. Hill and D. Hopkinson, *J. Membr. Sci.*, 2018, **545**, 292-300.
76. D. Liu, J. Gui, L. Song, X. Zhang and Z. Sun, *Pet. Sci. Technol.*, 2008, **26**, 973-982.
77. T. A. Saleh, S. A. Al-Hammadi, A. Tanimu and K. Alhooshani, *J. Colloid Interface Sci.*, 2018, **513**, 779-787.
78. S. S. Shah, I. Ahmad, W. Ahmad, M. Ishaq and H. Khan, *Energy Fuels*, 2017, **31**, 7867-7873.
79. C. D. Wilfred, C. F. Kiat, Z. Man, M. A. Bustam, M. I. M. Mutalib and C. Z. Phak, *Fuel Process. Technol.*, 2012, **93**, 85-89.
80. E. Yang, C. Yao, Y. Liu, C. Zhang, L. Jia, D. Li, Z. Fu, D. Sun, S. Robert Kirk and D. Yin, *Fuel*, 2018, **211**, 121-129.

View Article Online
DOI: 10.1039/C8GC01615A

81. M. Zhang, W. Zhu, H. Li, M. Li, S. Yin, Y. Li, Y. Wei and H. Li, *Colloids and Surfaces A: Physicochemical and Engineering Aspects*, 2016, **504**, 174-181.
82. S. A. Dharaskar, K. L. Wasewar, M. N. Varma, D. Z. Shende and C. K. Yoo, *Ind. Eng. Chem. Res.*, 2014, **53**, 19845-19854.
83. U. Domańska and M. Wlazło, *Fuel*, 2014, **134**, 114-125.
84. M. Zarrabi, M. H. Entezari and E. K. Goharshadi, *RSC Adv.*, 2015, **5**, 34652-34662.
85. B. Avvaru, N. Venkateswaran, P. Uppara, S. B. Iyengar and S. S. Katti, *Ultrason. Sonochem.*, 2018, **42**, 493-507.

1